

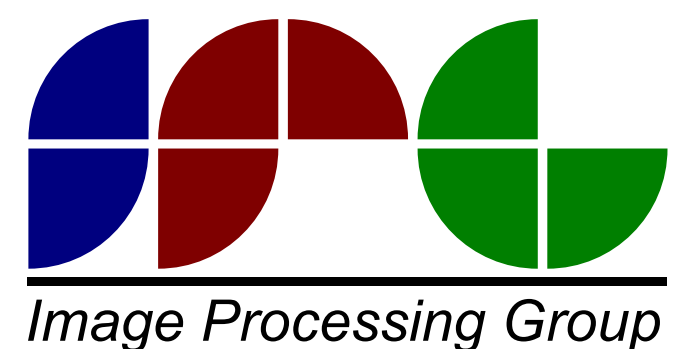
Modelling Periodic Motion for Background Subtraction in X-Ray Imaging



Tomislav Petković (tomislav.petkovic.jr@fer.hr)

Sven Lončarić (sven.loncaric@fer.hr)

University of Zagreb Faculty of Electrical Engineering and Computing
Unska 3, HR-10000, Zagreb, Croatia



Abstract

Real-time guidewire segmentation in fluoroscopic images is a necessary prerequisite for automated monitoring and navigation systems to support minimally invasive endovascular interventions. We propose a background model that is specifically adapted to the X-ray modality and that is able to model periodic background movement, for example induced by heartbeat or breathing. The proposed background model requires about 1-2 periods of the periodic background motion to learn the motion parameters and can then be used to segment objects of interest such as guidewires or needles. We demonstrate the feasibility of the proposed method on one recorded X-ray sequence.

Conclusion

We have presented a background model that is able to capture the periodic movement of the background in X-ray fluoroscopic imaging. The model requires one to two periods of periodic movement to infer the parameters of the background motion and can then be used to segment objects of interest such as guidewires and needles. Obtained segmentation is directly usable in existing guidewire and needle navigational systems that are described in the literature as it complements spatial segmentation techniques by directly identifying relevant moving structures and thus enables removal of stationary anatomical line-type structures. Potential applications include cardiac or abdominal endovascular interventions where guidewires, catheters or needles are used. However, further work is required to validate the method on a larger set of X-ray sequences where the ground truth is known.

1 X-Ray Imaging Model

If a homogeneous and isotropic object is placed between the X-ray source and the detector then the observed intensity can be approximated as (narrow energy band, no beam diffusion) [Hasegawa, 1987, Schram, 2001]

$$I = I_0 \exp\left(-\sum_i \mu_i d_i\right) = I_0 \prod_i \gamma_i \quad (1-1)$$

where $\mu_i [\text{cm}^{-1}]$ is the linear attenuation coefficient and γ_i is the multiplicative attenuation factor of an i th object on the X-ray path. Any factor of the quantity $\prod_i \gamma_i$ may model an object of interest (guidewire, contrast agent, stents and instruments). Let γ_{gw} denote the multiplicative term of the guidewire. Then for pixels where the guidewire is absent we observe the intensity

$$I_1 = I_0 \prod_i \gamma_i, \quad (1-2)$$

and for pixels where the guidewire is present we observe the intensity (thin guidewire assumption)

$$I_2 = \exp(-\mu_{\text{gw}} d_{\text{gw}}) I_0 \prod_i \gamma_i = \gamma_{\text{gw}} I_1. \quad (1-3)$$

2 Kalman Filter

Proposed model is an extension of the stationary background model presented in [Petković and Lončarić, 2010]. We use the Kalman filter to learn the periodic motion and model the background. Let $i[n]$ be observed X-ray intensity at single pixel. Proposed model uses multiple states $\mathbf{b}[n]$ per pixel:

$$\begin{aligned} \mathbf{b}[n] &= \mathbf{b}[n-1] + \mathbf{Q}_1[n] \\ i[n] &= \mathbf{H}[n] \mathbf{b}[n] + Q_2[n] \end{aligned} \quad (2-1)$$

where $\mathbf{b}[n]$ is a vector encoding background properties, \mathbf{Q}_1 is process noise, \mathbf{Q}_2 is measurement noise (R_1 and R_2 are noise autocorrelations), and $\mathbf{H}[n]$ is time-dependent matrix. State vector $\mathbf{b}[n]$ is a vector containing the Fourier series expansion of the observed periodic background:

$$\mathbf{b}^T = [b_0 \quad b_1 \quad b_{-1} \quad b_2 \quad b_{-2} \quad \dots \quad b_k \quad b_{-k} \quad \dots], \quad (2-2)$$

where the first element b_0 encodes the DC component of the background and the k th pair (b_k, b_{-k}) encodes the amplitude and phase of the k th harmonic. The measurement matrix $\mathbf{H}[n]$ is a row vector

$$\mathbf{H}[n] = [1 \quad \mathbf{O}_1 \quad \mathbf{O}_2 \quad \dots \quad \mathbf{O}_k \quad \dots], \quad (2-3)$$

where

$$\mathbf{O}_k = [\cos(\omega_p k t_n) \quad \sin(\omega_p k t_n)]. \quad (2-4)$$

Matrix $\mathbf{H}[n]$ models both the periodic behavior of the background and encodes the guidewire position. If the guidewire is absent then the measurement matrix $\mathbf{H}[n]$ is a row vector given by Eq. (2-3). If the guidewire is present then $\mathbf{H}[n]$ is simply multiplied by the guidewire attenuation factor γ_{gw} . The product $\mathbf{H}[n] \mathbf{b}[n]$ shows how the measured intensity $i[n]$ is decomposed using the Fourier series as:

$$i[n] = b_0 + \sum_{k=1}^{\infty} b_k \cos(\omega_p k t_n) + b_{-k} \sin(\omega_p k t_n). \quad (2-5)$$

Frequency ω_p determines the base frequency of the input signal decomposition into the Fourier series. If ω_p is known, e.g. provided by EKG or similar measurement), then the model (2-1) is linear and the Kalman filter is directly applicable. If ω_p is not known then there are two possible solutions: (1) the model of Eq. (2-1) is extended by assuming the constant frequency,

$$\omega_p[n] = \omega_p[n-1] + Q_3, \quad (2-6)$$

where Q_3 is the process noise, and extended Kalman filter (EKF) or unscented Kalman filter (UKF) are used to jointly track $\mathbf{b}[n]$ and ω_p ; (2) if the limit to the number of terms N is defined then the discrete Fourier transform in $2N+1$ points may be used instead of the truncated Fourier series.

3 Proposed Algorithm

The steps of the proposed background model are as follows (spatial coordinates are omitted for clarity):

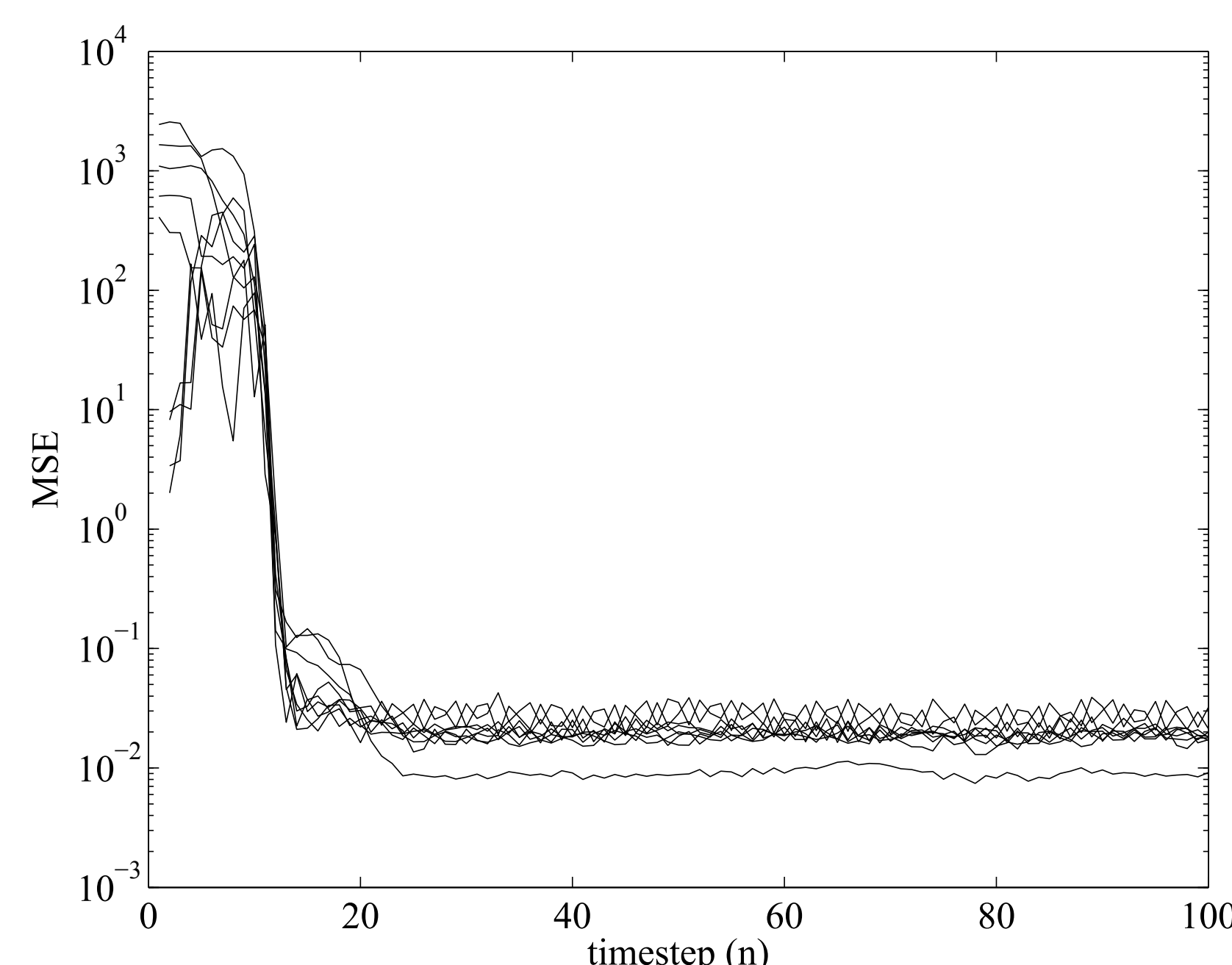
1. Compute the MAP estimate $b_{\text{MAP}}[n]$ from the input image to remove image dependent Poisson noise.
2. Segment the guidewire as follows:
 - (a) Compute the ratio between $b_{\text{MAP}}[n]$ and the background estimate $\hat{b}^-[n]$ given by the Kalman filter.
 - (b) Threshold the ratio image to segment the guidewire.
 - (c) Use the guidewire segmentation to set the measurement term $\mathbf{H}[n]$ of the Kalman filter.
3. Proceed with the Kalman filtering (EKF or UKF) using the model given by Eq. (2-1) (and Eq. (2-6)).

4 Results

We have performed one simulation experiment to estimate the speed of convergence of the Kalman filter and one experiment on the recorded patient data to demonstrate the feasibility of the proposed method.

4-1 Speed of Convergence

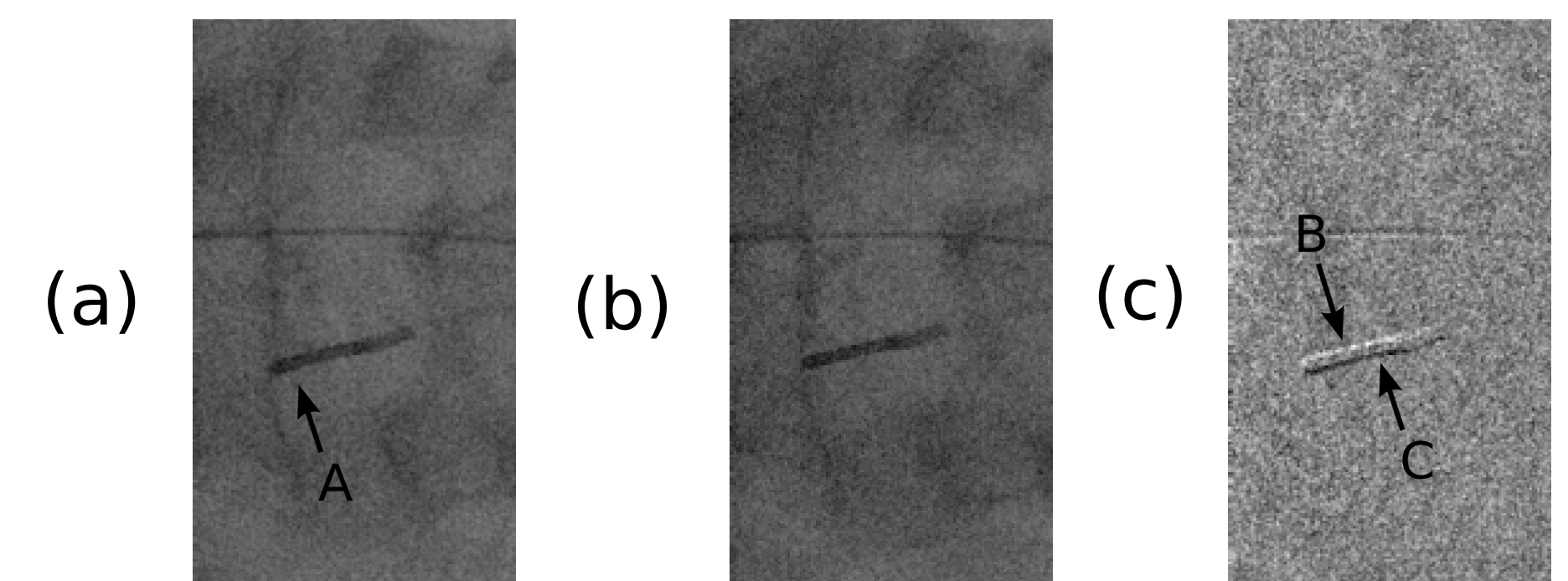
First experiment uses simulated background on a 20×20 grid using $N=4$ (nine Fourier components) where background amplitude is given by $b[x, y, n] = 128 + 64 \cos(k(x+y) - \omega_p t_n) + 32 \sin(k(x+y)/2 - 3\omega_p t_n) + w$, where $K=1/2$ is wave number, $\omega_p=1$ is frequency, and w is pixel-independent white noise. Ground truth decomposition is $b_0=128$, $b_1=64 \cos(k(x+y))$, $b_{-1}=64 \sin(k(x+y))$, $b_3=32 \sin(k(x+y)/2)$, and $b_{-3}=-32 \cos(k(x+y)/2)$; all other b_k are zero.



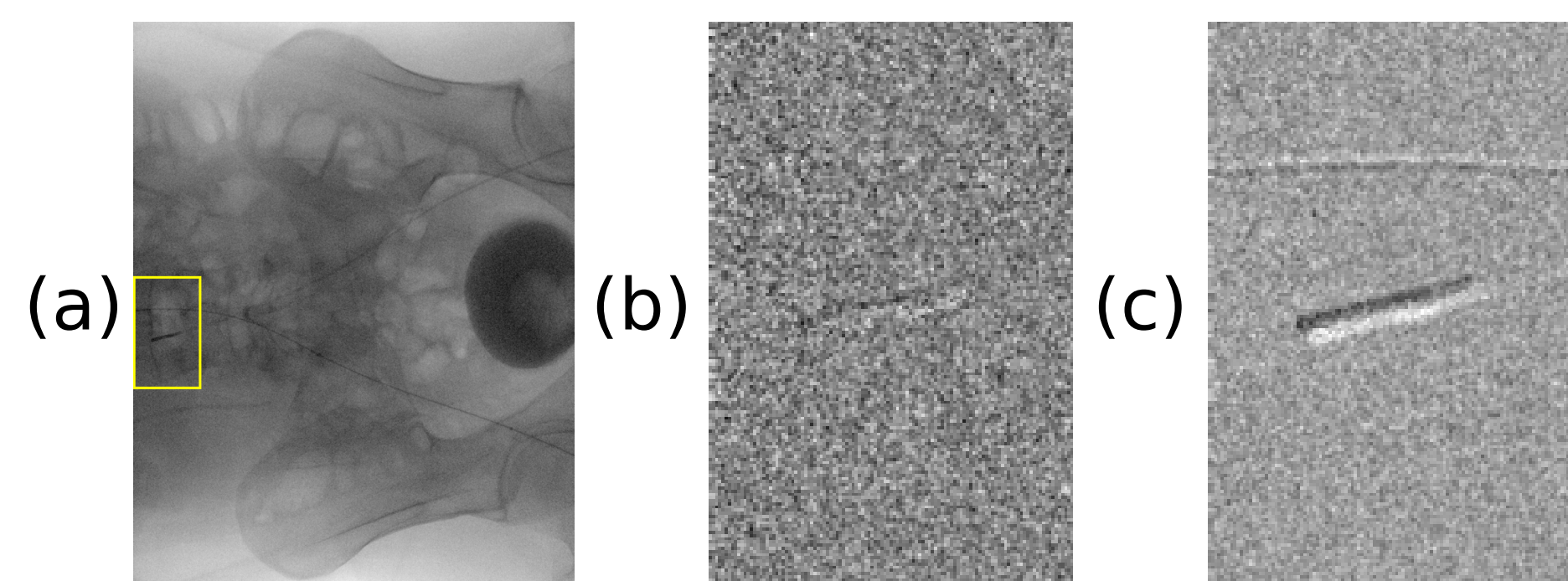
The mean squared error (MSE) for all nine background components is shown; note the MSE is large until the time-step 13 when it steeply decreases and then stabilizes around the time-step 23. This behavior is expected: MSE cannot decrease until at least one period of the motion is recorded (minimum of $2N+1=9$ samples), and after the first period the estimates are continuously corrected as additional samples are accumulated. About 1 to 2 additional periods are required to correctly estimate the noise. Effectively, the proposed method “learns” the background motion for every pixel independently. Therefore, the proposed model requires sufficiently long sequence that captures at least several periodic movements that are required for the Kalman filter to reach the steady state.

4-2 X-Ray Sequence

Second experiment uses a recorded X-ray sequence of an endovascular intervention in the abdominal aorta. The sequence has 145 frames of 1024×792 pixels at 12 bits. About 13 pulsations due to heartbeat are visible during the sequence therefore about 26 to 39 frames are needed to learn the motion. Segmentation validation for frames 40–145 was performed yielding FPR = 0.06 and TPR = 0.83.



Two X-ray images showing abdominal intervention; A is an opaque guidewire tip. Movement between (a) and (b) was due to breathing and heart beat. (c) is the simple difference; due to involuntary movement of the opaque tip A there are two strong false responses B and C.



Example MSE error for frame 62 of 145. (a) is 62nd frame; ROI is marked. (b) is enlarged difference for marked ROI using the proposed background model. (c) is enlarged difference for marked ROI using a simple time difference.

Acknowledgment

This work has been supported by the European Community Seventh Framework Programme under grant No. 285939 (ACROSS). The authors would like to sincerely thank Robert Homan of Philips Healthcare for provided X-ray images.

References

- References**
- [Baert et al., 2003] Baert, S., Viergever, M., and Niessen, W. (2003). Guide-wire tracking during endovascular interventions. *Medical Imaging, IEEE Transactions on*, 22(8):965–972.
 - [Bismuth et al., 2009] Bismuth, V., Vancanberg, L., and Gorges, S. (2009). A comparison of line enhancement techniques: applications to guide-wire detection and respiratory motion tracking. In *Proc. SPIE*, volume 7259. SPIE.
 - [Hasegawa, 1987] Hasegawa, B. (1987). *Physics of Medical X-Ray Imaging*. Medical Physics Publishing Corporation, revision of 2nd edition.
 - [Palti-Wasserman et al., 1997] Palti-Wasserman, D., Burstein, A. M., and Beyar, R. P. (1997). Identifying and tracking a guide wire in the coronary arteries during angioplasty from x-ray images. *IEEE Transactions on Biomedical Engineering*, 44(2):152–164.
 - [Petković et al., 2014] Petković, T., Homan, R., and Lončarić, S. (2014). Real-time 3d position reconstruction of guidewire for monoplane x-ray. *Computerized Medical Imaging and Graphics*, 38(3):211–223.
 - [Petković and Lončarić, 2010] Petković, T. and Lončarić, S. (2010). Guidewire tracking with projected thickness estimation. In *2010 IEEE International Symposium on Biomedical Imaging: From Nano to Macro*, pages 1253–1256. IEEE, IEEE.
 - [Schram, 2001] Schram, R. P. C. (2001). *X-ray attenuation—application of X-ray imaging for density analysis*. Technical Report 20002/01.44395/1, NRG.
 - [Takemura et al., 2008] Takemura, A., Hoffmann, K. R., Suzuki, M., Wang, Z., Rangwala, H. S., Harauchi, H., Rudin, S., and Umeda, T. (2008). An algorithm for tracking microcatheters in fluoroscopy. *Journal of Digital Imaging*, 21(1):99–108.
 - [van Walsum et al., 2005] van Walsum, T., Baert, S., and Niessen, W. (2005). Guide wire reconstruction and visualization in 3DRA using monoplane fluoroscopic imaging. *Medical Imaging, IEEE Transactions on*, 24(5):612–623.
 - [Zarge and Corby, 1994] Zarge, J. A. and Corby, N. R. (1994). Method and apparatus for real-time tracking of catheter guide wires in fluoroscopic images during interventional radiological procedures. U.S. Patent 5,289,373. General Electric Company.